DOI: 10.1002/ejic.200900691

Carbodiphosphorane $C(PPh_3)_2$ as a Single and Twofold Lewis Base with Boranes: Synthesis, Crystal Structures and Theoretical Studies on $[H_3B\{C(PPh_3)_2\}]$ and $[\{(\mu\text{-}H)H_4B_2\}\{C(PPh_3)_2\}]^+$

Wolfgang Petz,*[a] Florian Öxler,[a] Bernhard Neumüller,*[a] Ralf Tonner,[a,b] and Gernot Frenking*[a]

Keywords: Boranes / Density functional calculations / Donor-acceptor systems / Bond energy / Ab initio calculations

The donor-acceptor complex $[(H_3B)\{C(PPh_3)_2\}]$ (**2**) has been synthesized by treating B_2H_6 with $C(PPh_3)_2$ and its geometry determined by X-ray structure analysis. Treatment of **2** with DME yields the complex $[\{(\mu\text{-}H)H_4B_2\}\{C(PPh_3)_2\}][B_2H_7]$ (**4**), which has also been isolated and structurally characterized. Compound **4** is the first complex of a carbodiphosphorane where the carbon donor atom binds with its two-electron lone pairs to two main-group Lewis acids larger than protons. This reaction is likely to occur via initial formation of $[(H_3B)_2\text{-}\{C(PPh_3)_2\}]$ (**6**), which subsequently reacts with B_2H_6, with loss of a hydride, to yield **4**. Quantum chemical calculations of **2**, $\mathbf{4}^+$ and **6** show that the carbon–boron bonds in these complexes are very strong, and analysis of the bonding situation using the EDA, NBO and AIM methods reveals typical bonding patterns between the divalent carbon(0) moieties and one or two Lewis acids. The carbon donor atom of the carbodiphosphorane moiety remains strongly negatively charged even in the cation $\mathbf{4}^+$.

1. Introduction

Neutral donor ligands with a lone electron pair at carbon play an important role in organometallic chemistry and can be divided into several types, depending on the coordination at the carbon atom. Carbon monoxide and isonitriles, both of which possess singly coordinated carbon, are well-known ligands with an sp-type carbon atom that mainly form complexes with low-valent transition metals of the type [M]←CO and [M]←CNR.[1] Fischer-type carbyne complexes can be similarly formulated with singly coordinated carbon donor atoms ($[M]^-\leftarrow CR^+$).[2] Complexes which have a naked carbon atom as ligand ([M]←C) are a recently synthesized novel type of carbon-donor compound.[3] These carbon complexes were found to be isolobal to CO.[4] In the series of sp^2-type carbon ligands, the isolable N-heterocyclic carbenes (NHC) have attracted much interest in recent years as σ-donors in numerous complexes which have found numerous applications in homogeneous catalysis.[5] The carbene fragments in the Fischer-type carbene complexes $[M]\leftarrow CR_2$ and in ylides, which are usually written as $R_2C{=}PR_3$,[6] are further examples of formally sp^2-type carbon ligands.[7] The donor-acceptor complexes $E\leftarrow CR_2{=}PR_3$ and $E\leftarrow CH_2{=}M(L)_x$, where E is a Lewis acid, are the only known compounds with an sp^3-carbon donor atom.[8]

The carbodiphosphorane $C(PPh_3)_2$ (**1**),[9] which has a strongly bent geometry, is an unusual carbon ligand.[10] In contrast to NHC compounds, **1** has *two* lone electron pairs at the divalent carbon(0) atom, which is stabilized by two phosphane groups through strong donor-acceptor bonds of the type L→C←L.[11] Carbodiphosphoranes are examples of CL_2 compounds where L is a strong σ donor.[12] The latter compounds have been termed carbones[13] to distinguish them from carbenes, which have only one lone electron pair. The related carbone $C(NHC)_2$, which contains benzoannelated NHC ligands instead of phosphanes, was recently synthesized and structurally characterized[14] after the geometry and stability of the parent carbodicarbene had been predicted by quantum chemical calculations.[15]

Since carbodiphosphoranes have two lone electron pairs at carbon, they should be able to bind either one Lewis acid E, to yield a complex of type **A** (Scheme 1), or two Lewis acids to give a complex of type **B** (Scheme 1). Some complexes of type **A** bound to Lewis acids containing group 13 atoms, such as the adducts of **1** with $InMe_3$ and $AlBr_3$, which have been characterized by X-ray analyses, are known.[16] Related adducts **A** with transition-metal[17] or other main-group Lewis acids[18] are also known. Similarly,

[a] Fachbereich Chemie der Philipps-Universität, Hans-Meerwein-Strasse, 35043 Marburg, Germany
E-mail: petz@staff.uni-marburg.de
neumuell@chemie.uni-marburg.de
frenking@staff.uni-marburg.de
[b] Centre for Theoretical Chemistry and Physics, New Zealand Institute for Advanced Study, Massey University Albany, Private Bag 102904, North Shore MSC, 0745 Auckland, New Zealand
Supporting information for this article is available on the WWW under http://www.eurjoc.org or from the author.

adducts of type **B** with two Lewis acids E are known in the cations $(H_2C\{PPh_3\}_2)^{2+}$, $[Ag\{HC(PPh_3)_2\}_2]^{3+}$,[11] $(HMeC\{PPh_3\}_2)^{2+}$[19] and in $[Cl_2Au_2\{\mu\text{-}C(PPh_3)_2\}]$.[20]

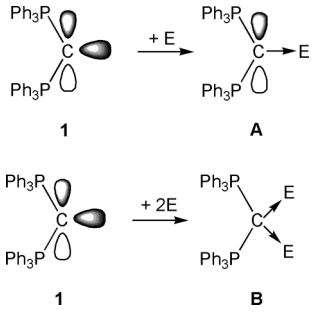

Scheme 1. Schematic representation of the bonding situation in carbodiphosphoranes and the change after complexation with (a) one and (b) two Lewis acids.

To date, no examples of a complex of type **B** where **1** binds two main-group Lewis acids other than a proton or proton/methyl are known. Somewhat surprisingly, no complex of type **A** with a boron-containing Lewis acid BX_3 has been isolated and structurally characterised either. The complex with the parent Lewis acid BH_3 is of particular interest as adducts of BH_3 with carbon-based Lewis bases are rare and crystal structures of carbon donors have only been published for an N-heterocyclic carbene[21] and an ylide,[22] although microwave structures have been reported for H_3BCO[23] and H_3BCNMe.[23] The latter species have also been studied by quantum chemical methods.[24] In 1981, for example, Schmidbaur and co-workers reported IR and NMR spectroscopic data for a BH_3 adduct with a cyclic carbodiphosphorane, although no structural data were reported.[25] Herein we report the first synthesis of a complex of **1** with the parent borane ligand BH_3 to be characterized by X-ray structure analysis. We also present experimental evidence for the synthesis of a complex where **1** binds two boron Lewis acids in the unusual adduct $[\{(\mu\text{-}H)H_4B_2\}\{C(PPh_3)_2\}][B_2H_7]$ (**4**). The results of quantum chemical calculations on these complexes and a bonding analysis of the compounds are also given.

2. Results

When a toluene solution of **1** was brought into contact with a bulb containing freshly prepared gaseous B_2H_6, colorless crystals formed at the surface of the solution after several days. These were subsequently identified as the addition compound $[H_3B\{C(PPh_3)_2\}]$ (**2**). For preparative purposes, B_2H_6 was bubbled, with stirring, into a solution of **1** in toluene to yield a yellowish precipitate; the reaction occurs immediately, even at low temperature. However, the result of this reaction is more complicated than a simple addition to give **2** directly. The resulting precipitate is presumably a mixture of compounds and is insoluble in toluene and other non-polar solvents. Further reaction occurs in polar solvents such as CH_2Cl_2, acetonitrile, and thf or related solvents, with gas evolution in most cases. Solvent reactions are typical for Lewis acid adducts of **1**, which makes spectroscopic characterization somewhat problematic and crystals for X-ray analyses difficult to obtain. Thus, if the precipitate is dissolved in dry DMSO gas evolution is observed and a main signal at δ = 21 ppm is found in the ^{31}P NMR spectrum. In order to understand these solvent reactions, we treated the precipitate with dry thf at room temperature. After gas evolution ceased, a colorless insoluble microcrystalline material had formed. The ^{31}P NMR spectrum of the solution showed three signals at δ = 39.4, 21.1, and 20.1 ppm in a 1:6:4 ratio. After allowing the mixture to stand for a couple of days, small colorless crystals were found to have grown along with larger yellow crystals. The colorless crystals were identified as the salt $(HC\{PPh_3\}_2)[B_3H_8]$ (**3**·THF), whereas the yellow crystals were found to be **2**·THF. Both compounds are only slightly soluble in thf. The ^{31}P NMR spectrum of the solute finally showed peaks at δ = 39.1 and 21.1 ppm in a 1:2.7 ratio. The crystals of **2**·THF are slightly soluble in DMSO, without gas evolution, and the ^{31}P NMR spectrum exhibits a singlet at δ = 21.00 ppm. To avoid reaction with a potential proton donor such as thf we treated the initial precipitate with dry dimethoxyethane (DME). A suspension was obtained, although in this case with little or no gas evolution. Small colorless crystals, which turned out to be the salt-like compound $[\{(\mu\text{-}H)H_4B_2\}\{C(PPh_3)_2\}][B_2H_7]$ (**4**), as shown by X-ray analysis, formed within several hours. The supernatant DME solution showed two signals in the ^{31}P NMR spectrum at δ = 39.4 and 21.2 ppm. Additionally to **4** a few other crystals could be isolated from DME, which turned out to be the salt $(HC\{PPh_3\}_2)[BH_4]$ (**5**). The proton in **5** probably comes from internal redox processes during the formation of B–B bonds and H_2.

The unusual behavior of the initial precipitate indicates that **3** and **4** are not formed in the first reaction step but are solvent-induced consecutive products. We therefore suppose that the precipitate from **1** and B_2H_6 in toluene consists of a mixture of **2** and the bis-adduct $[(H_3B)_2\{C(PPh_3)_2\}]$ (**6**). The latter product is considered to be highly reactive and responsible for the gas evolution in protic solvents. Quantum chemical calculations suggest that both the mono-adduct **2** and the bis-adduct **6** are stable at ambient temperature as the BH_3 group is small enough to allow two ligands to be attached to the two lone electron pairs of **1** with formation of a type **B** compound.[12b] The isolation of **4** may be a hint that the predicted adduct **6**, which subsequently undergoes the observed reaction, is the main product in toluene. This is supported by the fact that only the initial toluene precipitate gives gas evolution upon dissolution in DMSO; the products **2**, **3**, and **4** obtained from thf or DME only dissolve. However, to date we have been unable to confirm or to exclude the presence of **6**. The salt-like adduct **4** is the first compound of type **B** in which **1** coordinates to main-group Lewis acids in a bridging manner. This adduct can be considered to be derived from **6** by abstraction of a hydride ion, as shown in Scheme 2. We should point out here that the fragment $\{(\mu\text{-}H)H_4B_2\}^+$ is known from phosphane complexes.[26]

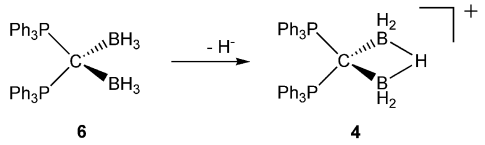

Scheme 2. Suggested reaction course for the formation of **4** from carbodiphosphorane and bis-borane.

The cation of **4** can also be seen as a formal derivative of B_2H_6 in which a bridging hydride species is replaced by the two-electron-pair donor **1** to yield a 14-electron $B_2H_5C^+$ fragment. A similar bonding situation is present in the unstable compounds B_2H_5X (X = halogen)[27] and in related fragments with X = P[26] or Fe.[28] The postulated bis-adduct **6** may abstract a proton from thf to finally produce the salt **3**, and dismutation into **2** and **4**, with hydride transfer to B_2H_6, may occur in DME.

The IR spectrum of **2** in Nujol mull shows medium strong absorptions at 2171, 2207, and 2257 cm^{-1} which are indicative for the B–H vibration of an end-on BH_3 group. In principle two stretching vibrations, with E and A_1 symmetry, are expected for ν_{as}(BH) and ν_s(BH), respectively. The three bands observed may arise from a symmetry reduction which causes the E vibration to split into two bands. Two strong bands at 1130 and 1143 cm^{-1} belong to BH_2 deformation vibrations.[29] The spectrum of **4** is more complicated and shows medium to strong bands for BH stretching vibrations between 2600 and 2210 cm^{-1}; BH_2 deformation vibrations appear at 1186 and 1175 cm^{-1} but cannot be assigned with certainty. The IR spectra of **3** and **5** are governed by the skeleton vibrations of the $(HC\{PPh_3\}_2)^+$ cation. The vibrational spectrum of **3** exhibits a broad and unresolved intense band at 2388 cm^{-1} and a less intense broad band at 2074 cm^{-1}, which can be assigned to the B–H stretching vibrations of the anion. Further medium intensity bands at 1059 and 1030 cm^{-1}, which do not arise from vibrations of the cation, are due to BH_2 deformation modes. The IR spectrum of **5** shows three strong and broad bands in the region of B–H stretching frequencies at 2280, 2214, and 2137 cm^{-1}, thus indicating that the T_d symmetry of the $[BH_4]^-$ anion is disrupted by the H···H contact to the cation. Additionally, a medium-strong band at 1078 cm^{-1} can be attributed to the BH_2 deformation vibration.[30]

Various ^{31}P NMR studies allowed us to assign the signals at δ = 39.4, 20.1, and 21.1 ppm from measurements in thf and DME to compounds **4**, **3**, and **2**, respectively.

Crystal Structures

X-ray analyses of **2**–**5** were performed to gain more insight into the structure of the complexes and their bonding situation. Colorless crystals of the solvent-free addition compound **2** were obtained by allowing a solution of **1** in toluene to stand under an atmosphere of B_2H_6 for several days. Yellow crystals of **2**·THF and small colorless crystals of **3**·THF were obtained from thf as described above. Very small crystals of **4** and needles of **5**·DME formed upon addition of DME to the crude product obtained from **1** and B_2H_6 in toluene. Details of the structure determination are summarized in the Experimental Section; bond lengths and angles are given in Tables 1, 2, 3, and 4. The molecular structures of **2** and **4** are depicted in Figures 1 and 2, respectively, whereas the structures of **3** and **5**, which contain known components, are not shown and will not be discussed further.

Table 2. Selected bond lengths [Å] and angles [°] in **3**·THF.

P(1)–C(1)	1.700(6)	P(1)–C(2)	1.810(6)
P(1)–C(8)	1.797(6)	P(1)–C(14)	1.810(6)
P(2)–C(1)	1.714(5)	P(2)–C(20)	1.817(6)
P(2)–C(26)	1.797(6)	P(2)–C(32)	1.803(6)
C(1)–H(1)	0.95	B(1)–B(3)	1.78(2)
B(1)–B(2)	1.79(2)	B(2)–B(3)	1.76(2)
C(1)–P(1)–C(2)	108.9(3)	C(1)–P(1)–C(8)	114.6(3)
C(8)–P(1)–C(2)	103.3(2)	C(1)–P(1)–C(14)	113.8(3)
C(8)–P(1)–C(14)	108.6(3)	C(2)–P(1)–C(14)	106.8(3)
P(1)–C(1)–P(2)	129.2(3)	P(1)–C(1)–H(1)	115.4
B(3)–B(1)–B(2)	59.1(6)	P(2)–C(1)–H(1)	115.4(2)
B(2)–B(3)–B(1)	60.7(7)	B(3)–B(2)–B(1)	60.2(7)

Table 1. Selected bond lengths [Å] and angles [°] in **2/2**·THF. Theoretical values at the BP86/SVP level of theory are given in italics.

P(1)–C(1)	1.681(3)/1.687(5)	*1.711*	P(1)–C(2)	1.825(2)/1.827(5)	*1.856*
P(1)–C(8)	1.832(3)/1.821(4)	*1.867*	P(1)–C(14)	1.803(3)/1.820(5)	*1.853*
P(2)–C(1)	1.689(3)/1.696(5)	*1.712*	P(2)–C(20)	1.818(3)/1.794(6)	*1.848*
P(2)–C(26)	1.838(3)/1.811(4)	*1.863*	P(2)–C(32)	1.806(3)/1.821(5)	*1.858*
C(1)–B(1)	1.673(4)/1.695(8)	*1.689*	B(1)–H(1)	1.12(3)/1.18(5)	*1.243*
B(1)–H(2)	1.21(4)/1.23(5)	*1.246*	B(1)–H(3)	1.14(3)/1.10(7)	*1.239*
C(1)–P(1)–C(2)	112.9(1)/113.1(2)	*110.9*	C(1)–P(1)–C(8)	113.2(1)/117.0(2)	*117.1*
C(1)–P(1)–C(14)	116.7(1)/115.3(2)	*116.9*	C(2)–P(1)–C(8)	105.7(1)/102.1(2)	*104.8*
C(2)–P(1)–C(14)	104.3(1)/102.3(2)	*103.8*	C(8)–P(1)–C(14)	102.9(1)/105.2(2)	*101.9*
C(1)–P(2)–C(20)	108.4(1)/113.4(2)	*109.1*	C(1)–P(2)–C(26)	116.2(1)/112.5(2)	*116.7*
C(1)–P(2)–C(32)	118.3(1)/117.8(2)	*117.8*	C(20)–P(2)–C(26)	107.3(1)/105.7(2)	*104.7*
P(1)–C(1)–P(2)	130.5(2)/125.1(3)	*128.2*	P(1)–C(1)–B(1)	117.3(2)/120.1(3)	*111.6*
P(2)–C(1)–B(1)	111.2(2)/114.1(4)	*118.7*	C(1)–B(1)–H(1)	113(1)/107(2)	*107.1*
C(1)–B(1)–H(2)	108(2)/115(2)	*111.5*	C(1)–B(1)–H(3)	114(3)/106(3)	*111.0*
H(1)–B(1)–H(2)	102(2)/113(3)	*109.2*	H(1)–B(1)–H(3)	107(2)/109(4)	*107.9*
H(2)–B(1)–H(3)	112(2)/107(4)	*109.9*			

Table 3. Selected bond lengths [Å] and angles [°] in the cation of **4**. Theoretical values for $\mathbf{4^+}$ at the BP86/SVP level of theory are given in italics.

B(1)–C(1)	1.67(2)	*1.644*	B(1)–B(2)	1.86(4)	*1.877*
B(1)–H(1)	1.30(18)	*1.348*	B(1)–H(2)	1.24(18)	*1.214*
B(1)–H(3)	1.19(16)	*1.208*	B(2)–C(1)	1.66(3)	*1.648*
B(2)–H(1)	1.40(20)	*1.347*	B(2)–H(4)	0.80(20)	*1.215*
B(2)–H(5)	1.30(29)	*1.216*	C(1)–P(1)	1.79(1)	*1.822*
C(1)–P(2)	1.80(1)	*1.829*	P(1)–C(8)	1.829(1)	*1.832*
P(1)–C(2)	1.829(3)	*1.842*	P(1)–C(14)	1.843(4)	*1.843*
P(2)–C(26)	1.826(5)	*1.842*	P(2)–C(20)	1.830(1)	*1.845*
P(2)–C(32)	1.842(8)	*1.835*			
C(1)–B(1)–B(2)	56(1)	*55.3*	C(1)–B(1)–H(1)	105(9)	*101.0*
B(2)–B(1)–H(1)	49(9)	*45.8*	C(1)–B(1)–H(2)	111(8)	*118.7*
B(2)–B(1)–H(2)	132(8)	*118.9*	H(1)–B(1)–H(2)	113(10)	*102.7*
C(1)–B(1)–H(3)	134(8)	*114.3*	B(2)–B(1)–H(3)	121(9)	*120.8*
H(1)–B(1)–H(3)	91(10)	*101.0*	H(2)–B(1)–H(3)	101(10)	*115.2*
C(1)–B(2)–B(1)	56(1)	*55.1*	C(1)–B(2)–H(1)	100(8)	*100.8*
B(1)–B(2)–H(1)	44(8)	*45.9*	C(1)–B(2)–H(4)	120(10)	*117.3*
B(1)–B(2)–H(4)	119(10)	*123.8*	H(1)–B(2)–H(4)	103(10)	*101.8*
C(1)–B(2)–H(5)	117(8)	*114.4*	B(1)–B(2)–H(5)	137(9)	*114.8*
H(1)–B(2)–H(5)	116(10)	*101.8*	H(4)–B(2)–H(5)	101(10)	*116.7*
B(2)–C(1)–B(1)	68(2)	*69.5*	B(2)–C(1)–P(1)	121(1)	*114.8*
B(1)–C(1)–P(1)	112(1)	*107.0*	B(2)–C(1)–P(2)	108(1)	*110.1*
B(1)–C(1)–P(2)	115(1)	*118.6*	P(1)–C(1)–P(2)	121.1(9)	*124.3*
C(1)–P(1)–C(8)	114.3(6)	*112.4*	C(1)–P(1)–C(2)	111.6(5)	*113.4*
C(1)–P(1)–C(14)	111.9(5)	*112.6*	C(1)–P(2)–C(26)	110.9(6)	*113.0*
C(1)–P(2)–C(20)	111.9(5)	*115.4*	C(1)–P(2)–C(32)	113.2(5)	*110.6*

Table 4. Selected bond lengths [Å] and angles [°] in **5**·DME.

C(1)–P(1)	1.697(3)	C(1)–P(2)	1.707(3)
C(1)–H(1)	0.85(3)	P(1)–C(8)	1.802(2)
P(1)–C(2)	1.822(2)	P(1)–C(14)	1.817(2)
P(2)–C(26)	1.796(3)	P(2)–C(32)	1.822(2)
P(2)–C(20)	1.816(2)	B(1)–H(2)	0.94(3)
B(1)–H(3)	1.05(3)	B(1)–H(4)	1.11(3)
B(1)–H(5)	1.02(4)		
P(1)–C(1)–P(2)	129.1(2)	P(1)–C(1)–H(1)	120(2)
P(2)–C(1)–H(1)	111(2)	C(1)–P(1)–C(2)	109.9(1)
C(1)–P(1)–C(8)	112.9(1)	C(1)–P(1)–C(14)	114.8(1)
C(1)–P(2)–C(20)	110.6(1)	C(1)–P(1)–C(26)	113.4(1)
C(1)–P(1)–C(32)	113.0(1)		

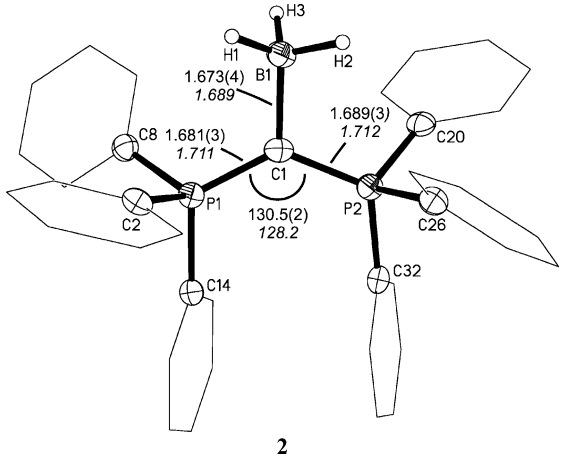

2

Figure 1. X-ray structure of $[H_3B\{C(PPh_3)_2\}]$ (**2**) showing bond lengths [Å] and angles [°]. Values calculated at the BP86/SVP level of theory are given in italics.

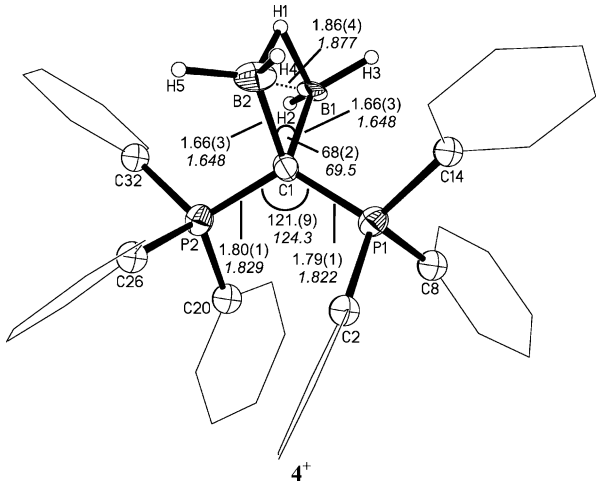

$\mathbf{4^+}$

Figure 2. X-ray structure of the cation of $\mathbf{4^+}$: $[\{(\mu\text{-H})H_4B_2\}\{C(PPh_3)_2\}]^+$ showing bond lengths [Å] and angles [°]. Values calculated at the BP86/SVP level of theory are given in italics.

Crystal Structure of 2

This compound crystallizes from toluene with no additional solvent molecules. The molecular structure is depicted in Figure 1. There are no close contacts between the individual molecules. The environment of the ylidic carbon atom C(1) is not exactly planar but shows a slight pyramidalization − the sum of the angles is 359.0(2)°. Theoretical calculations predict an angle of 358.5°. Thus, the C atom is located about 0.1 Å out of the plane containing the boron and the two phosphorus atoms. The B–C distance is 1.673(4) Å, which is about 0.07 Å longer than in the related

NHC adduct;[21] in both cases the boron atoms are bonded to sp^2-carbon atoms. The P–C bond lengths, which are very short in the starting compound **1** (1.61 Å) and correspond to a partial double bond, have a mean value of 1.685(3) Å, which is in the range of other $[X_3E\{C(PPh_3)_2\}]$ compounds.[16] The P–C–P angle of 130.5(2)° is close to that in the $(HC\{PPh_3\}_2)^+$ cations of **3** and **5**.

Crystal Structure of 2·THF

The thf molecule in the unit cell of **2**·THF is disordered over two positions, both of which could be refined. It has no close contacts to **2** and does not change the bonding parameters of the adduct shown in Figure 1 markedly. The slight pyramidalization at C(1) found in **2** is confirmed, with the sum of the angles at C(1) being 359.3°; the carbon atom lies 0.09 Å above the P_2B plane. The C(1)–B(1) bond length of 1.695(8) Å is even longer, whereas the P(1)–C(1)–P(2) angle is more acute by about 5°. In light of the higher measuring temperature (193 vs. 100 K for solvent-free **2**), the thermal ellipsoids of the atoms are larger.

Crystal Structure of 3·THF

The cation of the salt-like compound **3** exhibits no unusual bonding parameters.[16] The thf molecule forms an O···H contact to the proton of the ylidic carbon atom with a C(1)···O(1) distance of 3.38(1) Å. No further contacts exist between the cation and the $[B_3H_8]^-$ anion. Although numerous compounds with the $[B_3H_8]^-$ anion have been described,[31] only the crystal structure of the salt $[BzNMe_3][B_3H_8]$ is known;[32] the B–B distances in both compounds range between 1.76 and 1.80 Å.

Crystal Structure of 4

The unit cell of **4** contains two independent cations, the parameters of which differ only slightly. The molecular structure of one of the cations is depicted in Figure 2. The B–C distances are similar to those of **2** and **2**·THF. The P–C distances increase by about 0.12 Å on going from **2** to **4** and approach a normal single bond between an sp^3-carbon atom and a phosphorus atom. The carbon atom C(1) is in a distorted tetrahedral environment with a narrow B–C–B angle of 68(2)°, while the P–C–P angle is 121.1(8)°, a value which is similar to that in the dication $(H_2C\{PPh_3\}_2)^{2+}$[33] or the trication $[\{(Ph_3P)_2CH\}\rightarrow Ag\leftarrow\{HC(PPh_3)_2\}]^{3+}$,[11] but about 10° smaller than in the monocation $(HC\{PPh_3\}_2)^+$ and most of the type-**A** addition compounds such as **2** or related compounds.[16] When **1** bridges two Au atoms, as in $[Cl_2Au_2\{\mu\text{-}C(PPh_3)_2\}]$, this angle is slightly narrower than in **4**.[20] The B(1)–B(2) distance of 1.86(4) Å can be considered to be a nonbonding interaction; the carbon atom provides four electrons to stabilize the $B_2H_5^+$ cation. Similar compounds in which a hydride anion in B_2H_6 has been replaced by a four-electron donor are rare and include the anion $(\mu\text{-}\{Ar(BH_3)P\}B_2H_5)^-$[26] and the transition metal complex $[\mu\text{-}[CpFe(CO)_2]B_2H_5]$.[28] The B–B distances in these compounds are 2.00 and 1.77 Å, respectively; that of **4** lies in between these values.

Crystal Structure of 5·DME

The salt-like compound **5**·DME can be considered as being derived from **2** upon hydrogenation and splitting of the incoming H_2 into H^+ and H^- to form weak H···H bridges with a C(1)–B(1) distance of 4.082(4) Å. The bridge between the proton of the cation and a $[BH_4]^-$ anion demonstrates the weakly acidic character of this proton, which agrees with the strongly basic character of **1**. The molecular structure of the cation in **5** is very similar to that of the cation in **3** as no clear contacts exist to the solvent molecule. The B–H bond lengths vary between 0.98(3) and 1.11(3) Å. The other parameters of the $(HC\{PPh_3\}_2)^+$ cation are normal and similar to those found for **3** and other salts with this cation.[16]

3. Theoretical Studies

We calculated the mono- and bis-borane complexes $[H_3B\{C(PPh_3)_2\}]$ (**2**) and $[(H_3B)_2\{C(PPh_3)_2\}]$ (**6**) and the cation of the hydrogen-bridged complex $[\{(\mu\text{-}H)H_4B_2\}\{C(PPh_3)_2\}]^+$ (**4**$^+$) using DFT and ab initio methods. The calculated structures of **2** and **4**$^+$ closely match the results for the X-ray structure analysis (see Figures 1 and 2). Tables 1 and 3 give experimental and calculated values for other bond lengths and angles, all of which are in good agreement. The optimized structure of the experimentally unknown bis-borane complex **6** is shown in Figure 3.

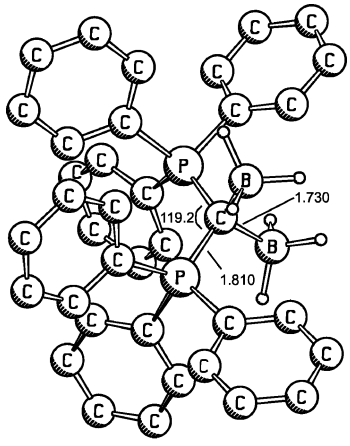

6

Figure 3. Optimized geometry of $[(H_3B)_2\{C(PPh_3)_2\}]$ (**6**) at the BP86/SVP level of theory showing calculated bond lengths [Å] and angles [°].

The data in Figures 1 and 2 indicate that the C–B bonds in cation **4**$^+$ are much shorter (1.644 Å) than in the neutral bis-borane complex **6** (1.730 Å). This is reasonable because the positively charged $B_2H_5^+$ ligand in **4**$^+$ should be a much stronger Lewis acid than neutral $(BH_3)_2$ in **6**. It is interesting to compare the calculated bond strength of the borane

Table 5. Calculated bond dissociation energies (BDEs) for the borane complexes **2**, **4**$^+$, and **6** (in kcal mol^{-1}).

Molecule	Ligand	BP86/TZVPP//BP86/SVP	MP2/TZVPP//BP86/SVP	SCS-MP2/TZVPP//BP86/SVP
$[H_3B\text{-}C(PPh_3)_2]$ (**2**)	BH_3	32.9	44.2	38.7
$[(H_3B)_2\text{-}C(PPh_3)_2]$ (**6**)	BH_3	23.0	33.2	27.0
$[(H_3B)_2C(PPh_3)_2]$ (**6**)	$(BH_3)_2$	55.9	77.4	65.7
$[\{(\mu\text{-}H)H_4B_2\}\{C(PPh_3)_2\}]^+$ (**4**$^+$)	$B_2H_5^+$	127.0	149.1	144.6

ligands in **2**, **4**, and **6**. The theoretically predicted bond dissociation energy (BDE) of the BH_3 ligand in **2** at the BP86/TZVPP//BP86/SVP level of theory is 32.9 kcal mol^{-1}, whereas the BDE of the $B_2H_5^+$ ligand in **4**$^+$ is 127.0 kcal mol^{-1} (Table 5). The calculated BDE of the second BH_3 ligand in **6** is still rather high at 23.0 kcal mol^{-1}, which gives a total bond energy for the borane ligands of 55.9 kcal mol^{-1}. The MP2 method gives higher BDEs, although they exhibit the same trend for all compounds investigated. The SCS correction, which is known to yield much more accurate bond energies,[34] brings the MP2 values of the BDEs closer to the BP86 results. All calculations indicate that the $B_2H_5^+$ ligand is very strongly bonded to the carbodiphosphorane.

Table 6 gives the atomic partial charges in **2**, **4**$^+$, and **6** in comparison with the parent carbodiphosphorane $C(PPh_3)_2$. The very large negative partial charge at the central carbon atom in $C(PPh_3)_2$ decreases slightly with increasing number of bonded boron atoms. However, there is still a negative charge of more than one electron at the central atom in **6** and even in the cation **4**$^+$. This observation can be understood by considering the bonding situation of the divalent carbon(0) compound in carbodiphosphorane and its complexes.[12b] The charge flow from the divalent C^0 atom to the Lewis acid is partly compensated by an increased charge flow from the phosphane ligands to carbon. The NBO method gives an optimized Lewis structure with a 2e,3c bond in the B1–H1–B2 moiety of **4**$^+$, which has an occupation number of 1.98 e. There are also two single bonds between C1 and the boron atoms with occupation numbers of 1.87 e as well as two single bonds between C1 and the phosphorus atoms with occupation numbers of 1.96 e, which are normal values for a tetracoordinate carbon atom.

For a more detailed discussion of the bonding situation it is useful to consider the hydrogen-substituted model compounds **4**$^+$**(H)** and **6(H)**. The most important geometrical parameters for these two compounds (see Figure 4) indicate that they are valid models for **4**$^+$ and **6**, in agreement with earlier studies on other carbone complexes.[12]

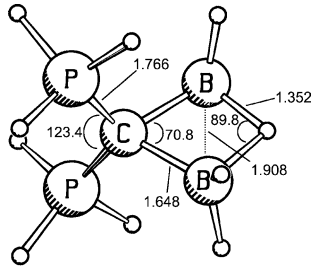

(a) **4**$^+$**(H)**

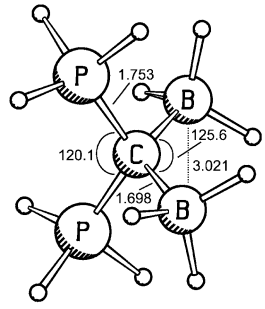

(b) **6(H)**

Figure 4. Optimized geometry of $[\{(\mu\text{-}H)H_4B_2\}\{C(PH_3)_2\}]^+$ (**4**$^+$**[H]**) (a) and $[(H_3B)_2\{C(PH_3)_2\}]$ (**6[H]**) (b) at the BP86/SVP level of theory showing calculated bond lengths [Å] and angles [°].

The EDA method gives an in-depth analysis of the donor–acceptor interactions in **4**$^+$**(H)** and **6(H)**. The numerical results are shown in Table 7. The very strong interaction energy (ΔE_{int}) between the borane ligand and the CDP is largely compensated in the cation **4**$^+$**(H)** by a high preparation energy that results from distortion of the $B_2H_5^+$ ligand from the triply bridged energy minimum structure. However, **4**$^+$**(H)** is much more strongly bonded than **6(H)**, as can be seen above for the real systems. The donor–acceptor interactions in **4**$^+$**(H)** and **6(H)** come mainly from the orbital term ΔE_{orb}, which is stronger in both these compounds than the electrostatic term ΔE_{elstat}. The breakdown

Table 6. Atomic partial charges (NBO) at the BP86/TZVPP//BP86/SVP level of theory for **2**, **4**$^+$, and **6**.

Molecule	q(B)	q(C)	q(P)	$q[C(PPh_3)_2]$
$C(PPh_3)_2$	–	–1.43	1.52	–
$[H_3B\text{-}C(PPh_3)_2]$ (**2**)	–0.45	–1.30	1.61/1.63	0.48
$[(H_3B)_2\text{-}C(PPh_3)_2]$ (**6**)	–0.43	–1.11	1.66	0.89
$[\{(\mu\text{-}H)H_4B_2\}\{C(PPh_3)_2\}]^+$ (**4**$^+$)	–0.24/–0.26	–1.12	1.66	0.15

of the orbital interactions into contributions which come from orbitals with different symmetry reveals interesting information about the donation of the σ and π lone-pair orbitals of the CDP. The molecules have C_{2v} symmetry, therefore donation of the σ lone-pair is associated with the $\Delta E_\sigma(a_1)$ term whereas donation of the π lone-pair is associated with the $\Delta E_{\pi\perp}(b_1)$ term. Figure 5 shows the relevant orbitals in **4⁺(H)**, which show up as HOMO-1 and HOMO-4. The rather small contributions from the $\Delta E_\delta(a_2)$ and $\Delta E_{\pi\parallel}(b_2)$ terms (Table 7) result from the donation of lower-lying occupied orbitals of $C(PH_3)_2$.

Table 7. EDA (BP86/TZ2P) results for complexes **4⁺(H)** and **6(H)**. The interacting fragments are the closed-shell Lewis base $C(PH_3)_2$ and the Lewis acids (LA) $B_2H_5^+$ and $(BH_3)_2$, respectively. Both compounds have been optimized with C_{2v} symmetry constraints. Energy values are given in kcal mol^{-1}. The P–C–P plane is defined as in-plane ($\pi_\perp$) while the B–C–B plane is defined as out-of-plane ($\pi_\parallel$).

	4⁺(H) → $B_2H_5^+$ + $C(PH_3)_2$		**6(H)** → 2 BH_3 + $C(PH_3)_2$	
ΔE_{int}	–222.4		–121.7	
ΔE_{Pauli}	293.1		284.5	
ΔE_{elstat}[a]	–209.8	(40.7%)	–185.4	(45.6%)
ΔE_{orb}[a]	–305.7	(59.3%)	–220.9	(54.4%)
$\Delta E_\sigma(a_1)$[b]	–192.5	(63.0%)	–94.6	(42.8%)
$\Delta E_\delta(a_2)$[b]	–4.5	(1.5%)	–8.1	(3.7%)
$\Delta E_{\pi\perp}(b_1)$[b]	–94.8	(31.0%)	–110.0	(49.8%)
$\Delta E_{\pi\parallel}(b_2)$[b]	–14.0	(4.6%)	–8.3	(3.7%)
ΔE_{prep}	111.0		46.4	
ΔE_{prep} (LA)	97.9		38.1	
ΔE_{prep} [$C(PH_3)_2$]	13.1		8.2	
ΔE (= $-D_e$)	–111.4		–75.4	

[a] The percentage values in parentheses give the contribution to the total attractive interactions $\Delta E_{elstat} + \Delta E_{orb}$. [b] The percentage values in parentheses give the contribution to the total orbital interactions ΔE_{orb}.

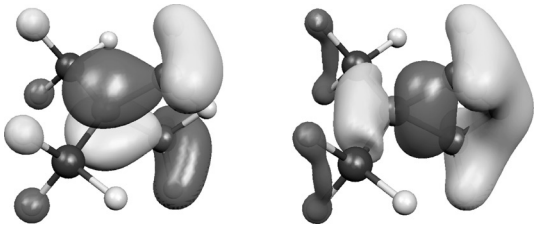

Figure 5. Molecular orbitals of **4⁺(H)** at the BP86/SVP level of theory showing the bonding interaction between $C(PH_3)_2$ and $B_2H_5^+$. HOMO-1 (left, –0.422 eV) and HOMO-4 (right, –0.502 eV).

The EDA results in Table 7 suggest that donation of the π lone-pair of the CDP moiety in **4⁺(H)**, which contributes 31.0% to ΔE_{int}, is only half as strong as the donation of the σ lone-pair, which contributes 63.0%. The π contribution becomes much more important in the neutral complex **6(H)**, however, where the $\Delta E_{\pi\perp}(b_1)$ term accounts for 49.8% of ΔE_{int} whereas the $\Delta E_\sigma(a_1)$ term accounts for only 42.8%. This can be explained by taking into account the geometry of the complexes − the H-bridged structure **4⁺(H)** has a very acute B–C–B angle of 70.8°, whereas the B–C–B angle in **6(H)** is 125.6°.

We also employed the Atoms-In-Molecules (AIM) method to elucidate the bonding situation in **4⁺(H)** and **6(H)**. Figure 6 shows the contour-line diagrams of the Laplacian $\nabla^2\rho(r)$ for the two molecules in the BCB plane.

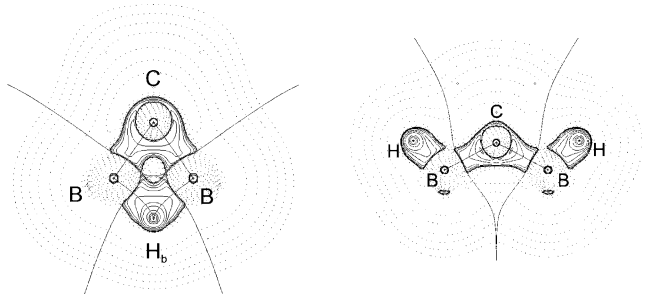

Figure 6. Contour-line diagrams [$\nabla^2\rho(r)$] for complexes **4⁺(H)** (left) and **6(H)** (right) in the BCB plane (BP86/TZVPP//BP86/SVP). Solid lines indicate areas of charge concentration [$\nabla^2\rho(r) < 0$] whereas dashed lines show areas of charge depletion [$\nabla^2\rho(r) > 0$]. The thick solid lines connecting the atomic nuclei are the bond paths. The thick solid lines separating the atomic basins indicate the zero-flux surfaces crossing the molecular plane.

The plots for both molecules show a region of charge concentration [$\nabla^2\rho(r) < 0$, solid lines] at the carbon atom which points towards the electron-deficient boron atoms. This is in agreement with the assignment of two donor orbitals at carbon. There are bond critical points and associated bond paths between carbon and both boron atoms in **4⁺(H)** and **6(H)**. In the former complex, bond paths are found between the boron atoms and the bridging hydrogen atom, although there is no B–B bond critical point. Instead, a ring critical point is found for the CB_2H moiety of **4⁺**.

In summary, the theoretical results clearly show that **4⁺** is the first main-group adduct of a carbodiphosphorane with two Lewis acids larger than protons where both lone-pairs of the CDP donor are engaged in donor–acceptor bonds. Furthermore, the bonding analysis shows that there are two carbon–boron bonds rather than a 2e,3c bond in **4⁺**.

4. Summary

The results of this work can be summarized as follows. The donor–acceptor complex [$(H_3B)\{C(PPh_3)_2\}$] (**2**) has been synthesized by treating B_2H_6 with $C(PPh_3)_2$ in toluene and its geometry determined by X-ray structure analysis. Treatment of the insoluble precipitate from this reaction with DME yields the complex [$\{(\mu\text{-}H)H_4B_2\}\{C(PPh_3)_2\}$]-[$B_2H_7$] (**4**), which was also isolated and structurally characterizeds. Compound **4** is the first complex of a carbodiphosphorane where the carbon donor atom binds to two main-group Lewis acids larger than protons through its two-electron lone pairs. It is likely that the reaction takes place after initial formation of [$(H_3B)_2\{C(PPh_3)_2\}$] (**6**), which subsequently reacts with B_2H_6, with loss of H^-, give **4**. Quantum chemical calculations on **2**, **4⁺**, and **6** have shown that the carbon–boron bonds in these complexes are very strong.

Analysis of the bonding situation using the EDA, NBO, and AIM methods has revealed a typical bonding pattern between divalent carbon(0) compounds and one or two Lewis acids. The carbon donor atom of the CDP moiety remains strongly negatively charged even in the cation $\mathbf{4}^+$.

5. Experimental Section

General: All operations were carried out under argon in dried and degassed solvents using Schlenk techniques. The solvents were thoroughly dried and freshly distilled prior to use. IR spectra were recorded with a Nicolet 510 spectrometer and ^{31}P NMR spectra with a Bruker AC 200 spectrometer. Elemental analyses were performed by the analytical service of the Fachbereich Chemie der Universität Marburg. Compound **1** was prepared from $(ClC\{PPh_3\}_2)Cl$ and $P(NMe_2)_3$ according to a modified literature procedure.[35] B_2H_6 was prepared as described previously.[36]

CCDC-736303 (for **2**), -736304 (for **2**·THF), -737305 (for **3**·THF), -736306 (for **4**), and -736307 (for **5**·DME) contain the supplementary crystallographic data for this paper. These data can be obtained free of charge from The Cambridge Crystallographic Data Centre via www.ccdc.cam.ac.uk/data_request/cif; see also Table 8.

Reaction of 1 with B_2H_6: In a Schlenk tube, 0.29 g of **1** (0.53 mmol) was layered with approx. 5 mL of toluene. Due to the low solubility of **1** in cold toluene, only a dilute solution formed. Without stirring, the Schlenk tube was connected to a flask filled with freshly prepared B_2H_6. Slow diffusion of gaseous borane into the solution resulted, after about one week, in the formation of colorless, needle-like crystals of **2** in the upper part of the Schlenk tube in low yields. The crystals of **2** were separated mechanically from unreacted crystals of **1**.

In a similar procedure, a slow stream of gaseous B_2H_6 was passed through a stirred solution of 1.56 g of **1** (2.92 mmol) in 10 mL of toluene at room temperature for about half an hour. A colorless to pale-yellow precipitate formed immediately, and the mixture was stirred mechanically for another hour. The precipitate was then filtered off and dried in vacuo to give a microcrystalline powder. Analysis for **2**. $C_{37}H_{33}BP_2$ (550.38): calcd. C 80.74, H 6.04. For **6**: $C_{37}H_{36}B_2P_2$ (564.21): calcd. C 78.76, H 6.43; found C 76.73, H 7.09. IR (Nujol mull): $\tilde{\nu}$ = 2683 (w), 2537 (w), 2461 (m), 2392 (s br), 2211 (m), 2041 (m br), 1588 (w), 1481 (m), 1435 (s), 1312 (w), 1265 (m), 1260 (m), 1186 (w), 1142 (m), 1103 (s), 1061 (m), 1032 (s), 999 (m), 955 (w), 947 (w), 800 (m), 748 (s), 720 (s), 692 (s), 625 (w), 607 (w), 544 (m), 543 (s), 523 (m), 502 (s) cm^{-1}. The IR spectrum of the precipitate from toluene does not contain bands belonging to the cation $(HC\{PPh_3\}_2)^+$, which forms in contact with polar solvents such as thf or DME. This cation must therefore form upon treatment of the precipitate with these solvents, as described below.

The precipitate of this reaction is insoluble in nonpolar hydrocarbons such as benzene, toluene, or hexane. For further characterization, attempts were made to dissolve the precipitate in polar solvents such as DCM, thf, DME, DMSO, and others. In all cases gas evolution was observed and the results upon contacting the precipitate with various solvents are as follows:

CH_2Cl_2: The product dissolved in DCM with gas evolution. The ^{31}P NMR spectrum of the solution exhibits signals at δ = 38.4, 36.5, and 20.3 ppm in a 1:3:6 ratio; the latter signal can be attributed to the cation $(HC\{PPh_3\}_2)^+$.

THF: Addition of 2 mL of dry thf to about 100 mg of the precipitate caused gas evolution and a suspension was obtained. The mixture was stirred mechanically for several minutes and was then allowed to stand at room temperature. The ^{31}P NMR spectrum of the supernatant solution showed three signals at δ = 39.4, 21.1, and 20.1 ppm in a 1:6:4 ratio, which were attributed to $\mathbf{4}^+$, **2**, and $(HC\{PPh_3\}_2)^+$, respectively. Two sorts of crystals, which were separated mechanically, grew upon allowing the suspension to stand for several days. The majority of these crystals were colorless crystals of the salt-like compound **3**·THF and a few were orange crystals of **2**·THF. The crystals of **2**·THF are only slightly soluble in DMSO (no gas evolution was observed) and exhibit a singlet at δ = 21.0 ppm in the ^{31}P NMR spectrum. **2·THF:** IR (Nujol mull): $\tilde{\nu}$ = 2293 (w br), 2257 (m), 2207 (m), 2170 [s; all ν(BH)], 1481 (m), 1435 (s), 1142 (s), 1130 (s), 1103 (s), 1061 (m), 1030 (w), 891 (m), 820 (w), 750 (s), 710 (m), 694 (m), 532 (m), 525 (w), 519 (m), 511 (w), 500 (m) cm^{-1}. **3·THF:** IR (Nujol mull) $\tilde{\nu}$ = 2386 (s br), 2045 [m br; all ν(BH)], 1478 (m), 1437 (s), 1312 (w), 1232 (m), 1182 (w), 1161 (w), 1138 (w), 1098 (s), 1072 (m), 1059 (m), 1030 (s), 1013 (s), 991 (s), 908 (m), 804 (m), 766 (m), 750 (s), 743 (s), 720 (s), 712 (s), 700 (s), 694 (s), 689 (s), 559 (s), 540 (s), 517 (s) cm^{-1}.

DME: Addition of 2 mL of DME (freshly dried with potassium) to about 120 mg of the precipitate caused only slight gas evolution and a suspension was obtained. The supernatant solution showed signals at δ = 39.6 and 21.5 ppm in a 1:6 ratio, which were assigned to $\mathbf{4}^+$ and **2**, respectively; a very small signal at δ = 20.6 ppm is probably due to the cation $(HC\{PPh_3\}_2)^+$. Small crystals, which turned out to be the salt-like complex **4**, separated upon allowing the suspension to stand for several days. A DMSO solution of the crystals of **4** exhibits a singlet at δ = 37.5 ppm; two further signals with very low intensities at δ = 21.4 and 20.9 ppm were assigned to **2** and the cation $(HC\{PPh_3\}_2)^+$, respectively. **4:** IR (Nujol mull): $\tilde{\nu}$ = 2507 (w), 2456 (m), 2417 (m), 2240 (s), 2211 [s; all ν(BH)], 1481 (w), 1464 (s), 1435 (s), 1186 (m), 1175 (m), 1144 (m), 1099 (s), 1069 (w), 1040 (m), 1026 (m), 999 (w), 986 (w), 872 (w), 762 (w), 748 (m), 739 (w), 714 (s), 693 (s), 534 (s), 525 (s), 507 (s), 498 (m) cm^{-1}. Further large crystals found in the DME suspension were found to be the salt **5**·DME. IR (Nujol mull): $\tilde{\nu}$ = 2280 (s), 2213 (s), 2135 [m, $\nu(BH_4)$], 1478 (m), 1435 (s), 1366 (w), 1236 (m), 1190 (m), 1101 (s), 1076 (m), 1032 (m), 1013 (m), 991 (s), 855 (m), 808 (m), 770 (m), 762 (m), 745 (s), 716 (s), 694 (s), 559 (s), 544 (s), 519 (m), 494 cm^{-1} (m). The bands at 1032, 1013, and 991 cm^{-1} are typical for the cation $(HC\{PPh_3\}_2)^+$; salts with this cation are scarcely soluble in DME.

DMSO: The toluene precipitate dissolved in DMSO with gas evolution. The ^{31}P NMR spectrum showed a single signal at δ = 20.8 ppm.

Dioxane: The precipitate is only slightly soluble in dioxane and the supernatant solution exhibited singlets at δ = 39.6, 25.0, and 21.2 ppm in a 2:0.1:2.4 ratio. No crystals separated upon standing for several days.

Acetone: The precipitate dissolved with gas evolution and the solution showed a singlet at δ = 19.7 ppm in the ^{31}P NMR spectrum.

Acetonitrile: The ^{31}P NMR spectrum of the supernatant solution showed seven signals (relative intensities in brackets) at δ = 19.37 (7.7), 19.87 (2.1), 20.71 (2.8), 21.41 (4.4), 22.25 (7.7), 23.60 (11.8), 24.40 (6.0), and 36.0 (1.0) ppm. After 18 h only the signals at δ = 19.37 (2.0), 19.87 (1.0), and 21.41 ppm (1.8) remainedd.

Theoretical Methods: Geometry optimizations without symmetry constraints were carried out using the Gaussian03 optimizer[37] together with TurboMole5[38] energies and gradients at the BP86[39]/def-SVP[40] level of theory. A minimal basis set (benzene BS) was used for the phenyl rings of the PPh_3 groups, except for the α-C

Table 8. Crystal data and structure-refinement details.

	2	**2**·THF	**3**·THF	**4**	**5**·DME
Formula	$C_{37}H_{33}BP_2$	$C_{41}H_{41}BOP_2$	$C_{41}H_{47}B_3OP_2$	$C_{37}H_{42}B_4P_2$	$C_{41}H_{45}BO_2P_2$
Mw [g mol^{-1}]	550.43	622.54	650.20	591.89	642.52
a [Å]	11.942(1)	16.205(2)	12.251(2)	12.794(2)	9.865(1)
b [Å]	16.756(2)	10.941(1)	12.298(2)	34.484(9)	19.727(1)
c [Å]	15.200(2)	18.669(2)	13.797(2)	16.256(3)	18.509(1)
α [°]	90	90	69.93(2)	90	90
β [°]	101.56(1)	93.05(1)	69.44(2)	104.65(2)	99.94(1)
γ [°]	90	90	74.47(2)	90	90
Crystal size [mm]	$0.3 \times 0.22 \times 0.08$	$0.49 \times 0.34 \times 0.32$	$0.22 \times 0.11 \times 0.06$	$0.12 \times 0.12 \times 0.06$	$0.28 \times 0.19 \times 0.06$
Volume [pm$^3 \times 10^6$]	2979.8(6)	3305.3(6)	1802.3(5)	6939(2)	3547.9(4)
Z	4	4	2	8	4
$d_{calcd.}$ [g cm^{-3}]	1.227	1.251	1.198	1.133	1.203
Crystal system	monoclinic	monoclinic	triclinic	monoclinic	monoclinic
Space group	*Cc* (Nr. 9)	$P2_1/c$ (Nr. 14)	$P\bar{1}$ (Nr. 2)	$P2_1/c$ (Nr. 14)	$P2_1/c$ (Nr. 14)
Diffractometer	IPDS II (Stoe)	IPDS I (Stoe)	IPDS I (Stoe)	IPDS I (Stoe)	IPDS II (Stoe)
Radiation			Mo-K_α		
Temperature [K]	100	193	193	193	193
μ [cm^{-1}]	1.7	1.64	1.5	1.133	1.57
$2\theta_{max}$ [°]	52.08	52.96	52.40	52.46	51.84
Index range	$-14 \le h \le 14$	$-19 \le h \le 19$	$-15 \le h \le 15$	$-15 \le h \le 15$	$-12 \le h \le 11$
	$-20 \le k \le 20$	$-13 \le k \le 13$	$-15 \le k \le 15$	$-42 \le k \le 42$	$-24 \le k \le 24$
	$-18 \le l \le 18$	$-22 \le l \le 22$	$-17 \le l \le 16$	$-20 \le l \le 20$	$-22 \le l \le 22$
Reflections collected	17180	31691	17891	59536	25339
Independent reflections (R_{int})	5780 (0.078)	6313	6611 (0.1045)	13431 (0.8377)	6581 (0.0935)
Observed reflections					
[$F_o > 4\sigma(F_o)$]	4218	2499	2947	886	3903
Parameters	374	384	457	215	438
Absorption correction			numerical		
Structure solution	direct methods	direct methods	direct methods	direct methods	direct methods
	SHELXS-97[57]	SIR-92[58]	SIR-92[58]	SIR-92[58]	SIR-92[58]
Refinement against F^2			SHELXL-97[59]		
H atoms	H1, H2, H3	H1, H2, H3	H2 to H9 of $[B_3H_8]^-$	–	H1 to H5
	were refined free[a]	were refined free[a]	were refined free[a]		were refined free[a]
Flack parameter	0.09(8)	–	–	–	–
R_1	0.0376	0.0825	0.0827	0.0663	0.0451
wR_2 (all data)	0.0767	0.2224	0.2424	0.2562	0.0951
Max. residual electron density					
[10^{-6} e pm^{-3}]	0.18	0.57	1.03	0.165	0.262

[a] Calculated positions with common displacement parameter.

atom. Stationary points were characterized as minima by calculating the Hessian matrix analytically at this level of theory.[41] Kohn–Sham orbitals were taken from these calculations. Single-point energies for the BP86/def-SVP (hereinafter SVP) optimized geometries were calculated with the MP2 method[42] applying the frozen-core approximation for non-valence shell electrons and with BP86 using the def2-TZVPP[43] basis set (hereinafter TZVPP). The resolution-of-identity method was applied for the BP86 and MP2 calculations.[44] MP2 energies were also calculated including the spin-component-scaled (SCS) correction proposed by Grimme,[45] using the standard parameters. NBO[46] analyses were carried out with the internal module of Gaussian03 at the BP86/TZVPP level of theory. The electronic charge distribution was also analyzed using the Atoms-In-Molecules (AIM) method,[47] which was performed at the BP86/TZVPP level of theory with a locally modified version of the AIMPAC program package.[48]

For the bonding analysis, some molecules were optimized with a C_{2v} symmetry constraint using the ADF2006.01 program package.[49] As above, BP86 was chosen applying uncontracted Slater-type orbitals (STOs) as basis functions.[50] The latter basis sets for all elements have triple-ζ quality augmented by two sets of polarization functions (ADF-basis set TZ2P). Core electrons (i.e., 1s for second- and [He]2s2p for third-period atoms) were treated by the frozen-core approximation. This level of theory is denoted BP86/TZ2P. An auxiliary set of s, p, d, f, and g STOs was used to fit the molecular densities and to represent the Coulomb and exchange potentials accurately in each SCF cycle.[51] Scalar relativistic effects were incorporated by applying the zeroth-order regular approximation (ZORA) in all ADF calculations.[52]

The interatomic interactions were investigated by means of an energy decomposition analysis (EDA) developed independently by Morokuma[53] and by Ziegler and Rauk.[54] This bonding analysis focuses on the instantaneous interaction energy, ΔE_{int}, of a bond A-B between two fragments A and B in the particular electronic reference state and in the frozen geometry of AB. This interaction energy is divided into three main components; see Equation (1).

$$\Delta E_{int} = \Delta E_{elstat} + \Delta E_{Pauli} + \Delta E_{orb} \quad (1)$$

The term ΔE_{elstat} corresponds to the quasi-classical electrostatic interaction between the unperturbed charge distributions of the prepared atoms and is usually attractive. The Pauli repulsion, ΔE_{Pauli}, is the energy change associated with the transformation from the superposition of the unperturbed electron densities of the isolated fragments to the wave function, which properly obeys the Pauli principle through explicit antisymmetrization and renormalization

(N = constant) of the product wave function.[49a] ΔE_{Pauli} comprises the destabilizing interactions between electrons of the same spin on either fragment. The orbital interaction, ΔE_{orb}, accounts for charge transfer and polarization effects.[55] The ΔE_{orb} term can be decomposed into contributions from each irreducible representation of the point group of the interacting system. The molecules investigated show C_{2v} symmetry, which makes it possible to distinguish between σ-contributions (a_1) and π-contributions arising from in-plane (b_2) $\pi_{\parallel}$ orbitals and out-of-plane (b_1) $\pi_{\perp}$ orbitals. The energy contributions from orbitals which possess δ symmetry (a_2) are negligible for the investigated molecules; see Equation (2).

$$\Delta E_{orb}\ (C_{2v}) = \Delta E_{\sigma}(a_1) + \Delta E_{\delta}(a_2) + \Delta E_{\pi\perp}(b_1) + \Delta E_{\pi\parallel}(b_2) \quad (2)$$

To obtain the bond dissociation energy (BDE; by definition with the opposite sign to ΔE), the preparation energy, ΔE_{prep}, which gives the relaxation of the fragments into their electronic and geometric ground states, must be added to ΔE_{int}; see Equation (3).

$$\Delta E\ (= -\mathrm{BDE}) = \Delta E_{int} + \Delta E_{prep} \quad (3)$$

Further details regarding the EDA method and its application to analysis of the chemical bond[56] can be found in the literature.

Supporting Information (see footnote on the first page of this article): Table with the calculated geometries and energies of the molecules.

Acknowledgments

We thank the Deutsche Forschungsgemeinschaft (DFG) for financial support. W. P. is also grateful to the Max-Planck-Gesellschaft, Munich for financial support, and R. T. thanks the Alexander von Humboldt-Stiftung for financial support (postdoctoral fellowship).

[1] C. Elschenbroich, *Organometallchemie*, 4. ed., Teubner Verlag, Stuttgart, Leipzig, Wiesbaden, **2003**.
[2] S. F. Vyboishchikov, G. Frenking, *Chem. Eur. J.* **1998**, *4*, 1439.
[3] a) R. G. Carlsson, M. A. Gile, J. A. Heppert, M. H. Mason, D. R. Powell, D. Vander Velde, J. M. Vilain, *J. Am. Chem. Soc.* **2002**, *124*, 1580; b) A. Hejl, T. M. Trnka, M. W. Day, R. H. Grubbs, *Chem. Commun.* **2002**, 2524; c) S. R. Caskey, M. H. Stewart, J. E. Kivela, J. R. Sootsman, M. J. A. Johnson, J. W. Kampf, *J. Am. Chem. Soc.* **2005**, *127*, 16750; d) M. H. Stewart, M. J. A. Johnson, J. W. Kampf, *Organometallics* **2007**, *26*, 5102.
[4] a) A. Krapp, G. Frenking, *J. Am. Chem. Soc.* **2008**, *130*, 16646; b) A. Krapp, K. K. Pandey, G. Frenking, *J. Am. Chem. Soc.* **2007**, *129*, 7596.
[5] W. A. Hermann, T. Weskamp, V. P. W. Böhm, *Adv. Organomet. Chem.* **2002**, *48*, 1.
[6] A. W. Johnson, *Ylides and Imines of Phosphorus*, Wiley-Interscience Publication, New York, Chichester, Brisbane, Toronto, Singapore, **1993**.
[7] M. J. Calhorda, A. Krapp, G. Frenking, *J. Phys. Chem. A* **2007**, *111*, 2859.
[8] a) R. R. Schrock, *Acc. Chem. Res.* **1979**, *12*, 98; b) T. E. Taylor, M. B. Hall, *J. Am. Chem. Soc.* **1984**, *106*, 1576; c) N. Kuhn, A. Al-Sheikh, *Coord. Chem. Rev.* **2005**, *249*, 829 and references therein.
[9] F. Ramirez, N. B. Desai, B. Hansen, N. McKelvie, *J. Am. Chem. Soc.* **1961**, *83*, 3539.
[10] A. T. Vincent, P. Wheatley, *J. Chem. Soc., Dalton Trans.* **1972**, 617.
[11] W. Petz, B. Neumüller, G. Frenking, R. Tonner, *Angew. Chem.* **2006**, *118*, 8206; *Angew. Chem. Int. Ed.* **2006**, *45*, 8038 and references therein.
[12] a) R. Tonner, G. Frenking, *Chem. Eur. J.* **2008**, *14*, 3260; b) R. Tonner, G. Frenking, *Chem. Eur. J.* **2008**, *14*, 3273.
[13] a) R. Tonner, G. Heydenrych, G. Frenking, *ChemPhysChem.* **2008**, *9*, 1474; b) G. Frenking, R. Tonner, *Pure Appl. Chem.* **2009**, *81*, 597.
[14] C. A. Dyker, V. Lavallo, B. Donnadieu, G. Bertrand, *Angew. Chem.* **2008**, *120*, 3250; *Angew. Chem. Int. Ed.* **2008**, *47*, 3206.
[15] R. Tonner, G. Frenking, *Angew. Chem.* **2007**, *119*, 8850; *Angew. Chem. Int. Ed.* **2007**, *46*, 8695.
[16] W. Petz, C. Kutschera, S. Tschan, F. Weller, B. Neumüller, *Z. Anorg. Allg. Chem.* **2003**, *629*, 1235.
[17] a) W. Petz, F. Weller, J. Uddin, G. Frenking, *Organometallics* **1999**, *18*, 619; b) J. Sundermeyer, K. Weber, K. Peters, H. G. von Schnering, *Organometallics* **1994**, *13*, 2560; c) H. Schmidbaur, C. E. Zybill, G. Müller, C. Krüger, *Angew. Chem.* **1983**, *95*, 753; *Angew. Chem. Int. Ed. Engl.* **1983**, *22*, 729.
[18] a) H. Schmidbaur, C. E. Zybill, D. Neugebauer, *Angew. Chem.* **1982**, *94*, 321; *Angew. Chem. Int. Ed. Engl.* **1982**, *21*, 310; b) H. Schmidbaur, C. Zybill, D. Neugebauer, G. Müller, *Z. Naturforsch., Teil B* **1985**, *40*, 1293; c) W. Petz, C. Kutschera, B. Neumüller, *Organometallics* **2005**, *24*, 5038; d) W. Petz, F. Weller, C. Kutschera, M. Heitbaum, G. Frenking, R. Tonner, B. Neumüller, *Inorg. Chem.* **2005**, *44*, 1263.
[19] W. Petz, B. Neumüller, unpublished results.
[20] J. Vicente, A. R. Singhal, P. G. Jones, *Organometallics* **2002**, *21*, 5887.
[21] N. Kuhn, G. Henkel, T. Kratz, J. Kreutzberg, R. Boese, A. H. Maulitz, *Chem. Ber.* **1993**, *126*, 2041.
[22] a) H. Schmidbaur, G. Müller, B. Milewski-Mahrla, U. Schubert, *Chem. Ber.* **1980**, *113*, 2575; b) H. Schmidbaur, G. Müller, G. Blaschke, *Chem. Ber.* **1980**, *113*, 1480.
[23] A. C. Venkatacher, R. C. Taylor, R. L. Kuczkowski, *J. Mol. Struct.* **1977**, *38*, 17.
[24] J. F. Stevens Jr., J. W. Bevan, R. F. Curl Jr., R. A. Geanangel, M. Crace Hu, *J. Am. Chem. Soc.* **1977**, *99*, 1442.
[25] H. Schmidbaur, T. Costa, *Chem. Ber.* **1981**, *114*, 3063.
[26] V. L. Rudzevich, H. Gornizka, V. D. Romanenko, G. Bertrand, *Chem. Commun.* **2001**, 1634.
[27] *Holleman-Wiberg, Lehrbuch der Anorganischen Chemie*, 101. ed., Walter de Gruyter, Berlin, New York **1995**.
[28] T. J. Coffy, G. Medford, J. Plotkin, G. J. Long, J. C. Huffman, S. G. Shore, *Organometallics* **1989**, *8*, 2404.
[29] Gmelin, *Borwasserstoff Verbindungen*, vol. 18.
[30] Gmelin, *Handbook of inorganic chemistry boron compounds*, 1st suppl., vol. 1.
[31] Gmelin, *Handbook of inorganic chemistry B*, 4th suppl. vol. 1b and references therein.
[32] G. F. Mitchel, A. J. Welch, *J. Chem. Soc., Dalton Trans.* **1987**, 1017.
[33] W. Petz, M. Fahlbusch, E. Gromm, B. Neumüller, *Z. Anorg. Allg. Chem.* **2008**, *634*, 682.
[34] S. Grimme, *Acc. Chem. Res.* **2008**, *41*, 569.
[35] R. Appel, F. Knoll, H. Schöler, H.-D. Wihler, *Angew. Chem.* **1976**, *88*, 769; *Angew. Chem. Int. Ed. Engl.* **1976**, *15*, 701.
[36] *Handbuch der präparativen Anorganischen Chemie*, vol. 2 (Ed.: G. Brauer), F. Enke Verlag, Stuttgart, 3rd ed., **1978**.
[37] M. J. Frisch, G. W. Trucks, H. B. Schlegel, G. E. Scuseria, M. A. Robb, J. R. Cheeseman, J. A. Montgomery, Jr., T. Vreven, K. N. Kudin, J. C. Burant, J. M. Millam, S. S. Iyengar, J. Tomasi, V. Barone, B. Mennucci, M. Cossi, G. Scalmani, N. Rega, G. A. Petersson, H. Nakatsuji, M. Hada, M. Ehara, K. Toyota, R. Fukuda, J. Hasegawa, M. Ishida, T. Nakajima, Y. Honda, O. Kitao, H. Nakai, M. Klene, X. Li, J. E. Knox, H. P. Hratchian, J. B. Cross, V. Bakken, C. Adamo, J. Jaramillo, R. Gomperts, R. E. Stratmann, O. Yazyev, A. J. Austin, R. Cammi, C. Pomelli, J. W. Ochterski, P. Y. Ayala, K. Morokuma, G. A. Voth, P. Salvador, J. J. Dannenberg, V. G. Zakrzewski, S. Dapprich, A. D. Daniels, M. C. Strain, O. Farkas, D. K. Malick, A. D. Rabuck, K. Raghavachari, J. B. Foresman, J. V. Ortiz, Q. Cui, A. G. Baboul, S. Clifford, J. Cioslowski, B. B.

Stefanov, G. Liu, A. Liashenko, P. Piskorz, I. Komaromi, R. L. Martin, D. J. Fox, T. Keith, M. A. Al-Laham, C. Y. Peng, A. Nanayakkara, M. Challacombe, P. M. W. Gill, B. Johnson, W. Chen, M. W. Wong, C. Gonzalez, J. A. Pople, *Gaussian 03*, Revision D.01, Gaussian, Inc., Wallingford CT, **2004**.
[38] R. Ahlrichs, M. Baer, M. Haeser, H. Horn, C. Koelmel, *Chem. Phys. Lett.* **1989**, *162*, 165.
[39] a) A. D. Becke, *Phys. Rev. A* **1988**, *38*, 3098; b) J. P. Perdew, *Phys. Rev. B* **1986**, *33*, 8822.
[40] A. Schaefer, H. Horn, R. Ahlrichs, *J. Chem. Phys.* **1992**, *97*, 2571.
[41] P. Deglmann, F. Furche, R. Ahlrichs, *Chem. Phys. Lett.* **2002**, *362*, 511.
[42] a) C. Møller, M. S. Plesset, *Phys. Rev.* **1934**, *46*, 618; b) J. S. Binkley, J. A. Pople, *Int. J. Quantum Chem.* **1975**, *9S*, 229.
[43] F. Weigend, R. Ahlrichs, *Phys. Chem. Chem. Phys.* **2005**, *7*, 3297.
[44] a) K. Eichkorn, O. Treutler, H. Ohm, M. Häser, R. Ahlrichs, *Chem. Phys. Lett.* **1995**, *242*, 652; b) F. Weigend, *PCCP* **2006**, *8*, 1057.
[45] S. Grimme, *J. Chem. Phys.* **2003**, *118*, 9095.
[46] A. E. Reed, L. A. Curtiss, F. Weinhold, *Chem. Rev.* **1988**, *88*, 899.
[47] R. F. W. Bader, *Atoms in Molecules: A Quantum Theory*, Oxford University Press, Oxford, **1990**.
[48] a) AIMPAC, http://www.chemistry.mcmaster.ca/aimpac; b) A. Krapp, unpublished results.
[49] a) F. M. Bickelhaupt, E. J. Baerends, in: *Reviews in Computational Chemistry*, Wiley-VCH, New York, **2000**, vol. 15, pp. 1; b) G. te Velde, F. M. Bickelhaupt, E. J. Baerends, C. Fonseca Guerra, S. J. A. van Gisbergen, J. G. Snijders, T. Ziegler, *J. Comput. Chem.* **2001**, *22*, 931.
[50] J. G. Snijders, E. J. Baerends, P. Vernoojs, *At. Data Nucl. Data Tables* **1982**, *26*, 483.
[51] J. Krijn, E. J. Baerends, *Fit Functions in the HFS-Method*, Internal Report (in Dutch), Vrije Universiteit Amsterdam, The Netherlands, **1984**.
[52] a) E. Van Lenthe, E. J. Baerends, J. G. Snijders, *J. Chem. Phys.* **1993**, *99*, 4597; b) E. Van Lenthe, E. J. Baerends, J. G. Snijders, *J. Chem. Phys.* **1994**, *101*, 9783; c) E. Van Lenthe, A. Ehlers, E. J. Baerends, *J. Chem. Phys.* **1999**, *110*, 8943.
[53] K. Morokuma, *J. Chem. Phys.* **1971**, *55*, 1236.
[54] a) T. Ziegler, A. Rauk, *Inorg. Chem.* **1979**, *18*, 1755; b) T. Ziegler, A. Rauk, *Inorg. Chem.* **1979**, *18*, 1558.
[55] F. M. Bickelhaupt, N. M. M. Nibbering, E. M. Van Wezenbeek, E. J. Baerends, *J. Phys. Chem.* **1992**, *96*, 4864.
[56] a) G. Frenking, K. Wichmann, N. Fröhlich, C. Loschen, M. Lein, J. Frunzke, J. V. M. Rayón, *Coord. Chem. Rev.* **2003**, *238–239*, 55; b) M. Lein, G. Frenking, in: *Theory and Applications of Computational Chemistry: The First 40 Years* (Eds.: C. E. Dykstra, G. Frenking, K. S. Kim, G. E. Scuseria), Elsevier, Amsterdam, p. 367, **2005**; c) A. Krapp, F. M. Bickelhaupt, G. Frenking, *Chem. Eur. J.* **2006**, *12*, 9196.
[57] G. M. Sheldrick, *SHELXS-97*, University of Göttingen, Germany, **1997**.
[58] A. Altomare, G. Cascarano, C. Giacovazzo, A. Guagliardi, M. C. Burla, G. Polidori, M. Camalli, *Sir-92*, Rome, **1992**.
[59] G. M. Sheldrick, *SHELXL-97*, University of Göttingen, Germany, **1997**.

Received: July 1, 2009
Published Online: September 16, 2009

